Med Biol Eng Comput (2015) 53:645–653
DOI 10.1007/s11517-015-1260-4

ORIGINAL ARTICLE

Influence of first proximal phalanx geometry on hallux valgus deformity: a finite element analysis

Enrique Morales-Orcajo[1] · Javier Bayod[1] · Ricardo Becerro-de-Bengoa-Vallejo[2] · Marta Losa-Iglesias[3] · Manuel Doblare[1]

Received: 8 July 2013 / Accepted: 27 February 2015 / Published online: 18 March 2015

Abstract Hallux abducto valgus (HAV), one of the most common forefoot deformities, occurs primarily in elderly women. HAV is a complex disease without a clearly identifiable cause for its higher prevalence in women compared with men. Several studies have reported various skeletal parameters related to HAV. This study examined the geometry of the proximal phalanx of the hallux (PPH) as a potential etiologic factor in this deformity. A total of 43 cadaver feet (22 males and 21 females) were examined by means of cadaveric dissection. From these data, ten representative PPHs for both genders were selected, corresponding to five percentiles for males (0, 25, 50, 75, and 100 %) and five for females. These ten different PPHs were modeled and inserted in ten foot models. Stress distribution patterns within these ten PPH models were qualitatively compared using finite element analysis. In the ten cases analyzed, tensile stresses were larger on the lateral side, whereas compressive stresses were larger on the medial side. The bones of males were larger than female bones for each of the parameters examined; however, the mean difference between lateral and medial sides of the PPH (mean ± SD) was larger in women. Also the shallower the concavity at the base of the PPH, the larger the compressive stresses predicted. Internal forces on the PPH, due to differences in length between its medial and lateral sides, may force the PPH into a less-stressful position. The geometry of the PPH is a significant factor in HAV development influencing the other reported skeletal parameters and, thus, should be considered during preoperative evaluation. Clinical assessment should evaluate the first ray as a whole and not as isolated factors.

Keywords Hallux valgus deformity · Etiology · Gender differences · Proximal phalanx of the hallux · Finite element model

1 Introduction

Hallux abducto valgus (HAV) is one of the most common forefoot deformities, occurring more frequently in elderly women [32]. The symptoms associated with HAV are well known and can be summarized as lateral deviation of the big toe, increased angle between the first and second metatarsal (commonly known as a bunion), dislocation of the sesamoids, and muscle dysfunction [11]. These changes do not always correlate with each other, nor do they have the same intensity, rendering HAV a complex disease. In fact, there are more than 130 surgical procedures for the treatment of HAV which can be divided into soft tissue procedures, osteotomies, arthrodesis, arthroplasties, and combined procedures [20].

HAV is considered a deformity of multifactorial origin, primarily attributed to the use of footwear [23, 35], genetic conditions [22], and gender [40]. Additional factors also include metatarsus varus [18], abnormal length of the metatarsus [26] or abnormal shape of the metatarsal head [29], action of the foot muscles [34], and foot pronation [33].

✉ Javier Bayod
jbayod@unizar.es

[1] Group of Structural Mechanics and Materials Modeling (GEMM), Biomedical Research Networking Center in Bioengineering, Biomaterials and Nanomedicine (CIBER-BBN), Aragón Institute of Engineering Research (I3A), University of Zaragoza, Ed. Betancourt, C/María de Luna s/n, Saragossa, Spain

[2] Nursing Physiotherapy and Podiatry Faculty, Medicine Faculty, Complutense University, Madrid, Spain

[3] Faculty of Health Sciences, Rey Juan Carlos University, Madrid, Spain

Despite a large number of studies on this subject, the underlying cause of this deformity remains unclear. Even the use of footwear (commonly regarded as the primary suspect in HAV pathology) has not been confirmed as a cause. Barnicott and Hardy [3] measured the angle of the first metatarsophalangeal (MTP) joint in Nigerians who had never worn shoes and compared it with age-matched Nigerian soldiers who wore army boots. They found no significant differences in the angle of the MTP joint between the shod versus barefoot population. However, a significant difference was observed between men and women.

Using radiographs from pathologic versus non-pathologic male and female patients, several studies have focused on the skeletal parameters influencing HAV. Excessive length of the first metatarsal with respect to the second [19, 31, 37], also called protrusion [6, 18, 26, 28], has been associated with hallux valgus, but a short first metatarsal relative to the second [39] has also been suggested as an etiologic factor in HAV. Other reported etiologic factors include the shape of the metatarsal head [28, 29], a high intermetatarsal angle [18, 19], and hypermobility [25, 33]. Such a divergence of opinions regarding the etiology of HAV underscores the need for a new perspective in order to elucidate the underlying cause of this deformity.

Unlike previous studies, this study proposed the size and shape of the proximal phalanx of the hallux (PPH) as a skeletal parameter involved in HAV development. The underlying hypothesis involves abnormal stress on the PPH due to its shape (characterized by a larger length on the medial side compared with the lateral side), causing a tendency for the PPH to rotate. The effect of sexual dimorphism on the PPH was also evaluated to determine whether this factor predisposed women to suffer HAV pathology to a greater extent compared with men. The geometry of the PPH was examined by cadaveric dissection, and the stress state was predicted by FE analysis. In addition to provide a better understanding of this deformity, it is hoped that PPH geometry may provide an additional criterion by which physicians may gauge potential HAV severity.

2 Materials and methods

2.1 Proximal phalanx of the hallux (PPH) dissection and modeling

A total of 43 cadaver feet (22 males and 21 females) were examined by two surgeons (R.B.V. and L.I.) by means of cadaveric dissection. Data obtained from cadaveric dissection are common among surgeons as it allows quicker and easier collection of patient data, thereby obtaining a sufficient quantity of data [24]. Parameters that defined PPH geometry (Fig. 1) included longitudinal distance of the medial aspect (LDM), longitudinal distance of the central aspect (LDC), longitudinal distance of the lateral aspect (LDL), depth of the concave area at the base of the PPH (DCA), height of the base of the PPH (H), and width of the base of the PPH (W). All parameters involving each PPH examined were tabulated and divided by percentiles.

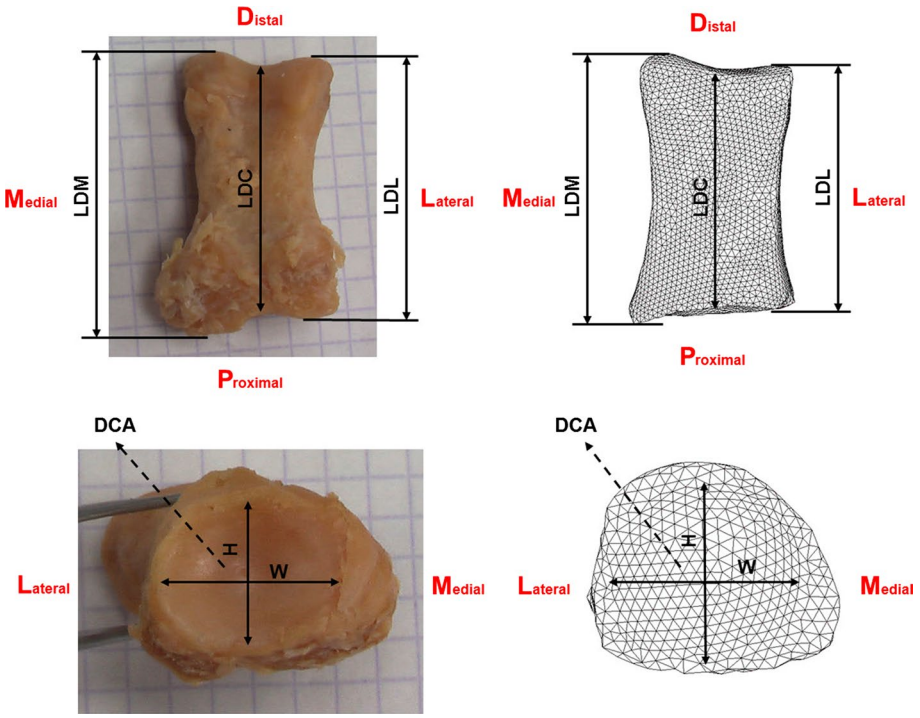

Fig. 1 Clinically significant PPH parameters. *LDM* longitudinal distance of the medial aspect, *LDC* longitudinal distance of the central aspect, *LDL* longitudinal distance of the lateral aspect, *DCA* depth of the concave area of the base of the PPH, *H* height of the base of the PPH, and *W* width of the base of the PPH

Table 1 Parameters used to model the new proximal phalanges sorted by percentiles of the dissected population

	LDM	LDC	LDL	DCA	H	W
M_0	30.52	28.76	29.04	3.57	16.51	20.93
M_25	31.18	31.54	31.33	1.56	16.39	22.39
M_50	36.5	35.39	35.04	3.08	23.21	24.53
M_75	40.31	33.01	36.51	1.25	17.78	21.35
M_100	38.51	37.91	38.4	2.21	15.56	20.72
W_0	31.23	29.00	29.5	1.27	14.08	17.51
W_25	31.71	30.48	30.86	0.72	13.23	17.66
W_50	34.45	30.15	32.63	0.66	12.33	19.04
W_75	38.64	34.24	35.34	2.32	17.26	17.72
W_100	40.16	39.35	42.78	2.42	18.7	20.00

LDM longitudinal distance of the medial aspect, *LDC* longitudinal distance of the central aspect, *LDL* longitudinal distance of the lateral aspect, *DCA* depth of the concave area of the base of the PPH, *H* height of the base of the PPH, and *W* width of the base of the PPH

Table 2 Material properties and element types used in the 3D finite element models

Component	Young's modulus (MPa)	Poisson coefficient	Type of element
Cortical bone	17,000	0.3	Tetrahedral
Trabecular bone	700	0.3	Tetrahedral
Ligaments	260	0.3	Tension-only truss
Plantar fascia	350	0.3	Tension-only truss
Cartilage	10	0.4	Tetrahedral
Muscles	450	0.3	Beam
Tendons	450	0.3	Tension-only truss

From this data set, five representative PPHs were selected for each gender, corresponding to five percentiles for males (0, 25, 50, 75, and 100 %) and five for females. These ten different PPHs were modified using parameters based on the data provided by surgeons. They were subsequently inserted into the FE foot model generating ten models which shared the same structure, differentiated only by PPH geometry. The parameters used to create each new proximal phalanx are shown in Table 1.

2.2 Finite element (FE) models

The FE geometry was obtained from a three-dimensional reconstruction of CT images of the right foot of a healthy male in his mid-thirties, and informed consent was obtained. CT images were acquired using a slice thickness of 2 mm. The FE meshes were constructed using commercial software HARPOON (Harpoon r1.4.5, CEI, Manchester, England). These meshes consisted of approximately 783,000 linear tetrahedrons with an average size of 1 mm which were determined after a mesh sensitivity analysis to ensure the convergence of the model [14]. The models were subsequently exported to the FE package, ABAQUS (ABAQUS 6.11.3, HKS, Pawtucket, RI).

Foot models consisted of 28 bones (talus, calcaneus, cuboid, navicular, three cuneiforms, five metatarsals, five proximal phalanges, four middle phalanges, five distal phalanges and two sesamoids), cartilage, nine ligaments (posterior talo-calcaneal, calcaneus, navicular, tarsometatarsal, and intermetatarsal, lisfranc, calcaneal cuboid-calcaneus-navicular, plantar and the plantar fascia), and nine tendons (extensor hallucis brevis, longus and capsularis, flexor digitorum brevis and longus, flexor hallucis brevis and longus, adductor and abductor halluces).

2.3 Material properties and boundaries

Seven different tissues were considered in our model, all idealized as homogeneous, isotropic, and linearly elastic materials (Table 2). Each bone was differentiated into cortical and trabecular bone [12, 14]. Ligaments were modeled using a tension-only, one-dimensional truss element that transmitted only axial forces, distinguishing between two types of material, i.e., stiffer ligaments (such as plantar fascia and superficial and deep plantar ligaments) and the remaining, more compliant ligaments [10]. Cartilage properties were selected from the literature [16]. The muscles were simulated with one-dimensional beam elements. In order to prevent moments at elements representing tendons, connections between muscles and bones were characterized as tension-only, one-dimensional elements, similar to ligaments [4, 27]. Joints were simulated by ligaments and cartilage which enabled free movement between bones during simulations [4]. Node to surface contact was used to prevent penetration between tendons and bones. The external face of the bone elements was defined as the master surface, whereas the slave surface was modeled with the nodes between the beams that represented the muscle.

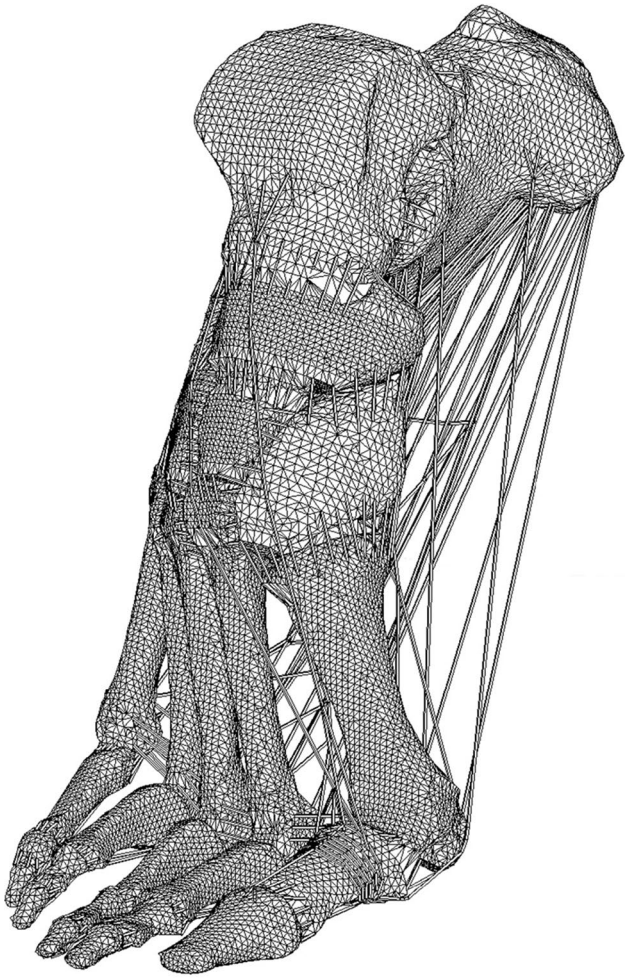

Fig. 2 Lateral view of the finite element model of a human skeleton right foot. The model was reproduced in toe-off position, forming a 90° angle between the metatarsals and phalanges

The position of the model was very important, since loads on the foot change in both direction and amplitude with each position. With this aim, Gefen et al. [17] proposed dividing the stance phase of gait into six different stages (initial-contact, heel-strike, mid-stance, forefoot-contact, push-off, and toe-off), defining loads values for each of these stages.

The best position to analyze the initial development stage of the hallux valgus deformity was the position where the metatarsal heads support their self-weight. According to the stance phases suggested by Gefen et al. [17], the model was positioned in the toe-off stage, forming an angle of 90° between the metatarsals and phalanges (Fig. 2).

In this position, the insertion of the Achilles tendon was considered as a fixed support, since this tendon generates most of the reaction force balancing the body weight. First and second phalanges were also considered as fixed support. For the remaining phalanges (third, fourth, and fifth toes), only the vertical movement was restricted [17]. In this position, the PPH displacement was fully restrained due to the position of the PPH in the foot structure at the particular stage of the gait cycle analyzed [17]. Furthermore, a load of 180.5 kg was applied to the joint surface formed by contact between tibia and fibula with the talus. This is the load that roughly corresponds to a subject with a body weight of 60 kg at this phase of gait. Also, at this stance phase, tendons were subjected to an initial pretension of 2 % to sustain the position in a resting state. Additional details on values and justifications used for loads and boundary conditions may be found in García-González et al. [15].

3 Results

3.1 Computer model predictions

For proper comparison, all models were ordered by size and gender. Gender was defined by a letter (M for males and W for females), and the percentile of the dissected population was characterized by a number (0 for the smallest phalanx and 100 for the largest one). Figure 3a shows the tensile stress distributions in the PPH, while Fig. 3b shows the compressive stress distributions. The stress distributions were similar for both men and women with a larger loaded area (appearing primarily in the larger phalanges) found in women compared with men. The tensile stresses (maximum principal) were mainly located in the lateral zone and the head of the PPH, whereas the compressive stresses (minimum principal) appeared mainly in the base and medial aspect of the PPH. Figure 4 shows the average tensile and compressive stress on both sides of PPH for each case analyzed. In all cases, tensile stresses were larger on the lateral side, whereas compressive stresses were larger on the medial side.

3.2 Phalanx dissection measurements

The measurements for the 43 PPH dissected are summarized in Table 3. Male bones were larger than female bones for each of the parameters examined in this study. However, the mean difference between the length of the lateral and medial sides of the large PPH (Mean + SD) in men was 1.87 mm, while this value was 2.40 mm in women, with the medial side being longer in both cases. In relative values, this difference was also proportionally larger in female phalanges. In large PPHs, the LDM compared with the LDL was 7 % larger in women, whereas it was only 5 % larger in men.

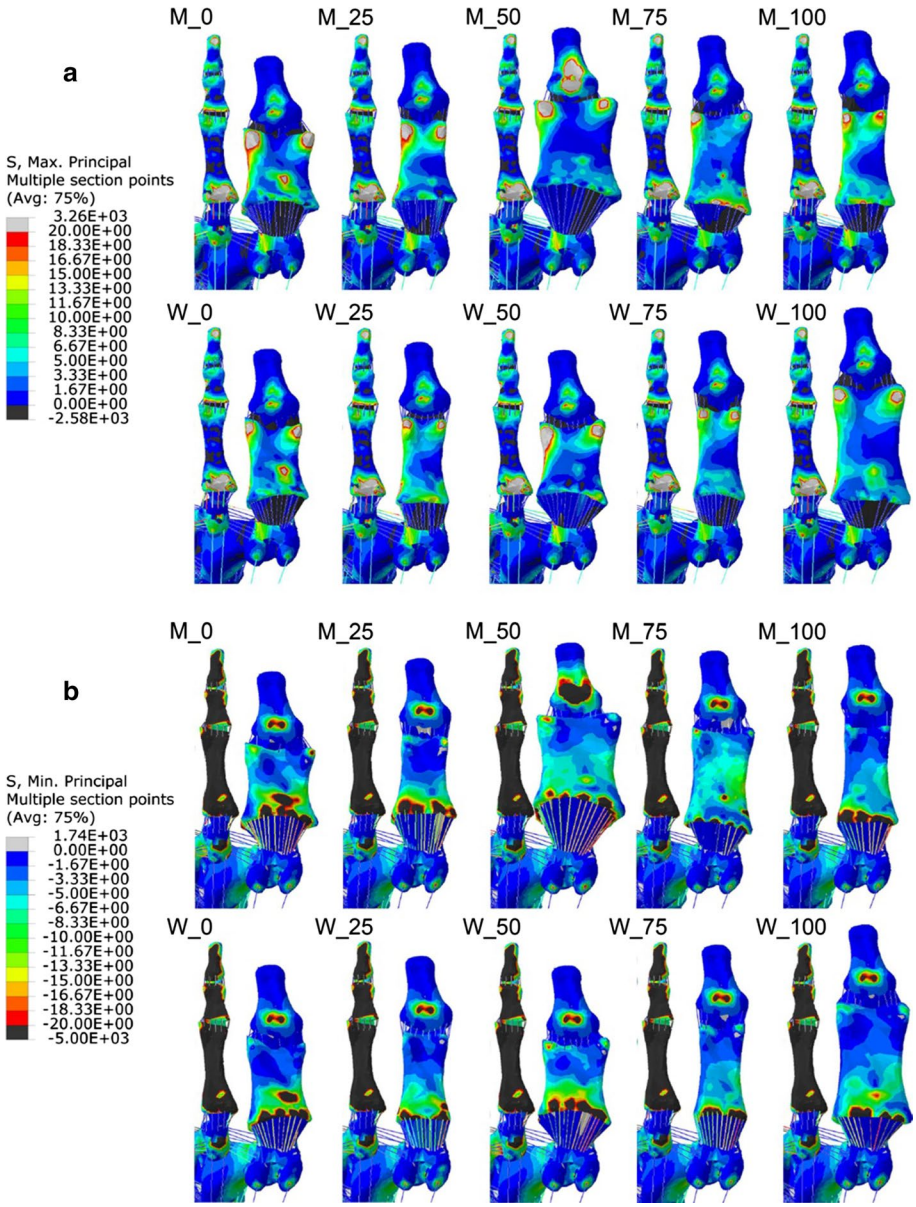

Fig. 3 Stress on the plantar area of the first and second radii of undeformed shape. **a** Tensile stress. **b** Compressive stress. The letter *M* corresponds to male gender, *W* corresponds to female gender, and the number corresponds to the percentile, with 0 being the smallest phalanx within the dissected population and 100 the largest one

$$1.051 = \frac{38.80}{36.93} < \frac{36.95}{34.55} = 1.070$$

According with the stress distribution, the medial side of the PPH in each model was compressed because of its length, whereas the lateral area was tensioned because it was shorter.

Stress differences were also found in the concavity at the base of the PPH where the metatarsal joint is located. In this area, a correlation between stress and DCA was observed, where the shallower the concave area, the larger the compressive stresses predicted (Fig. 5). It should be noted that compressive stresses in this area were doubled in magnitude and extent when compared with tensile stresses and were higher than the compressive stresses on the plantar face.

4 Discussion

In this paper, the geometrical characteristics of the PPH and their relationship to gender were analyzed for the first time. We gathered data from 43 cadaveric feet from healthy men and women. Subsequently, 10 representative cases were modeled by FE analysis. This enabled us to compare the stress distribution that occurs in the PPH in HAV.

It is very common to use the FE method to study foot pathology [9]. This technique provides an estimate of the mechanical stresses within the internal structures of the body that is often not directly measurable. In addition, the calculated stress distributions suggest where injury is likely to occur before it actually occurs.

Two FE studies related to HAV have been reported in the literature. The first study by Tao et al. [38] analyzed the influence of ligament laxity on the metatarsocuneiform joint of the first radius in HAV development. In addition, Matzaroglou et al. [30] compared the Chevron osteotomy at 60° and 90° as a treatment for HAV. Despite the statement by Tao et al. [38] that hypermobility helped in the adduction of the first metatarsal, neither of these two studies took into account the geometry of the PPH.

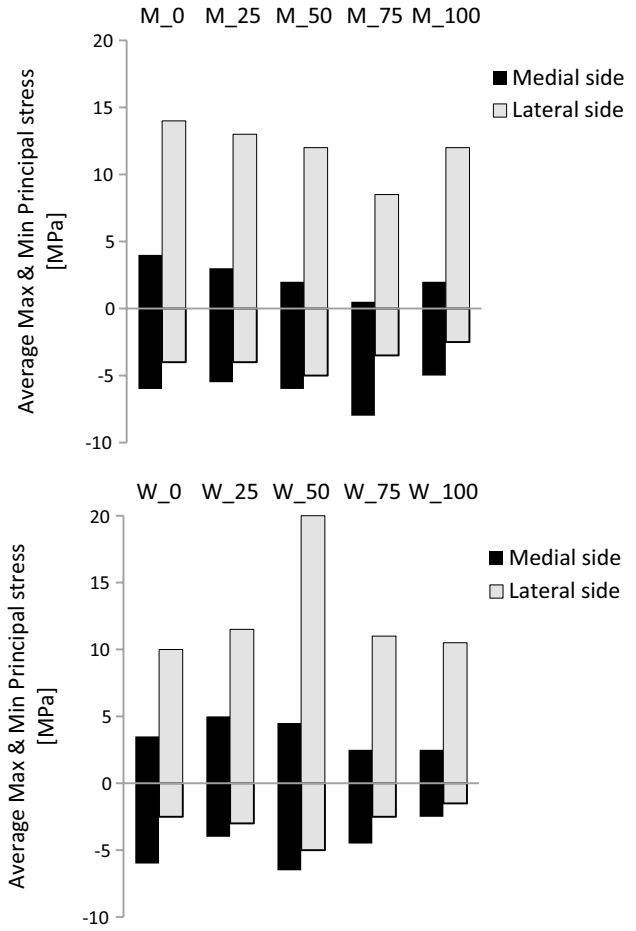

Fig. 4 Average tensile and compressive stresses at the medial and lateral sides of the PPH. The letter *M* corresponds to male gender, *W* corresponds to female gender, and the number corresponds to the percentile, with 0 being the smallest phalanx within the dissected population and 100 the largest one

This paper describes a new approach to understanding of HAV pathology from the perspective of the shape of the PPH. Prior research measured the length of the bones of first ray at the initial stage of HAV pathology for both male and female feet. Munuera et al. [31] concluded that the length of the metatarsal and the PPH in patients with HAV was higher than in non-pathologic cases. Using 98 non-pathologic feet, they reported an absolute mean PPH length of 32.70 ± 3.2 very similar to the 32.43 ± 2.3 measured in our population. Furthermore, in the figure they used to explain their method of measuring PPH length, they showed a representative PPH geometry. In that figure, it was easy to see the different lengths between medial and lateral sides of the PPH [31]. They also mentioned that the values of the variables between males and females were higher for male feet compared with female feet, which is consistent with our results. Measurements reported by Ferrari et al. [13] similarly noted that size was the main difference between male and female bones of the feet.

From earlier research, the shape of the first metatarsal head has also been considered an important anatomical feature of HAV. Mann and Coughlin [29] postulated that the shape of the first metatarsal head could be either square or rounded. A flattened metatarsophalangeal articulation would resist deforming forces much better than a rounded metatarsal head, which was thought to be highly prone to HAV development. This idea was also expressed by Mancuso et al. [28] in their study of the protrusion of the first metatarsal. They found a preponderance of rounded heads in their HAV population. The results from our simulations supported this hypothesis. The stresses in the concavity at the base of the PPH were larger for smaller depths (flatter heads) where opposition to rotation occurred. However, in deeper PPHs (rounded heads), lower stress levels were predicted (Fig. 5).

Table 3 Summary of data gathered from dissection

Variable (mm)	Male ($n = 22$)					Female ($n = 21$)				
	Min	Mean − SD	Mean	Mean + SD	Max	Min	Mean − SD	Mean	Mean + SD	Max
LDM	30.52	33.84	36.32	38.80	40.31	31.23	31.71	34.33	36.95	42.78
LDC	28.76	31.08	33.38	35.68	37.91	29.00	29.11	31.47	33.83	39.35
LDL	29.04	32.05	34.18	36.93	38.40	29.50	29.79	32.17	34.55	40.16
DCA	0.87	1.26	2.04	2.82	3.90	0.66	1.04	1.63	2.22	2.83
H	13.79	14.66	16.88	19.10	23.21	12.33	13.56	15.33	17.10	19.35
W	17.88	19.73	21.48	23.23	25.34	17.51	17.86	20.05	22.24	25.45

LDM longitudinal distance of the medial aspect, *LDC* longitudinal distance of the central aspect, *LDL* longitudinal distance of the lateral aspect, *DCA* depth of the concave area of the base of the PPH, *H* height of the base of the PPH, and *W* width of the base of the PPH

Our results suggested that the geometry of the PPH influenced its own stress pattern. The stresses estimated using the FE models were due to the difference in length between the medial and lateral sides. Stresses were tensile on the medial aspect of the PPH and compressive on the lateral aspect (Fig. 4). This stress pattern indicated an imbalance in the first ray. The internal forces within the PPH could then force a rotation of the PPH toward a more balanced position. Such a potentially less-stressful position involves rotation of the PPH laterally, so that the new configuration offsets the difference in lengths, thus relieving the stress. This rotation also causes separation of the metatarsals (Fig. 6).

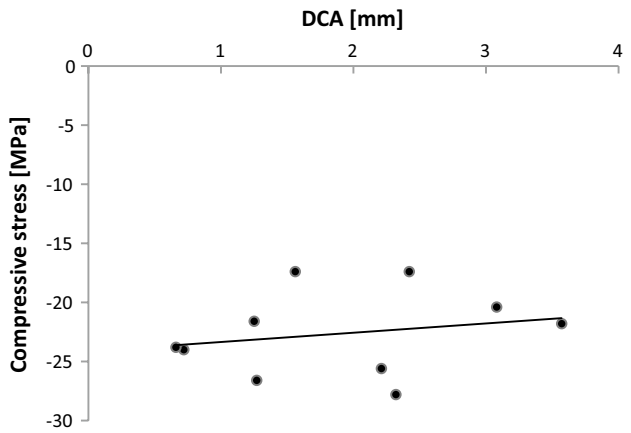

Fig. 5 Scatterplot and the trend line showing compressive stress at the PPH base versus depth of the concave area (DCA). *DCA* depth of the concave area of the base of the PPH

A similar idea was proposed by Ferrari et al. [13] but was expressed using angles to explain the differences in the angulation of the metatarsocuneiform joint between genders. They identified a significant difference in the angle of the facet on the metatarsal base with the medial cuneiform between men and women. Women had a greater angle, which caused a greater adduction of the metatarsal on the cuneiform compared with men [13]. In the case of the PPH base, the larger the differences in length between sides, the greater would be the abduction.

The rotation of the phalanx may be compounded by muscle function. No muscle inserts on the distal zone or head of the first metatarsal, nor on its middle area or diaphysis. The peroneus longus tendon is the only tendon that inserts on the proximal plantar area or on the base of the first metatarsal. In addition, the tibialis anterior tendon inserts on the medial and plantar area. By contrast, several tendons insert on the base of the proximal phalanx as follows: at its dorsal base, the tendon of the pedal muscle and tendon capsularis; at its plantar zone, two tendons from the short plantar flexor muscle; at its medial area, the adductor hallucis tendon; and at its lateral area, the tendon of the abductor hallucis muscle. Two tendons insert on the distal phalanx: one at the dorsal base (the extensor hallucis longus) and another at the plantar base (the flexor hallucis longus).

The electromyographic investigations performed by Iida and Basmajian [21] and Shimazaki and Takebe [34] found a weak medial flexion force against a stronger lateral flexion force in mild and severe HAV. Forces that markedly decreased abduction activity compared with

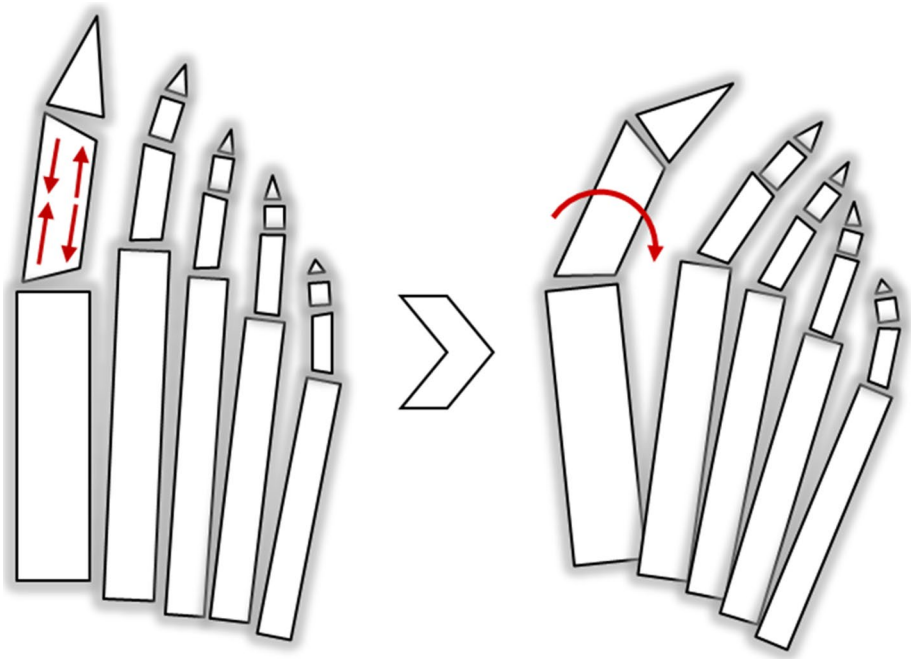

Fig. 6 Diagram demonstrating how the proximal phalanx rotates to reduce the stress

adduction were also reported in a much more recent electromyographic study [2], but none of these studies clarified whether this was a cause or a consequence of HAV. Thus, although it is still unclear whether muscle imbalance in first ray is the cause or just an aggravating factor in HAV development, there is evidence that muscle imbalance is related to the development HAV and could have a strong influence if other factors triggered rotation of the PPH.

Therefore, there must be some intrinsic predisposing factors (such as protrusion of the first metatarsal, shape of the head of the first metatarsal, metatarsocuneiform angulation, intermetatarsal angle, or the geometry of the PPH) that make some feet more vulnerable to HAV deformity than others. In addition, these factors are also affected by confinement forces exerted by footwear and the imbalanced forces of the muscular activity at the MTP joint. Future studies which investigate all these factors together, instead of examining each factor individually, are needed. Also, the influence of each factor on HAV development would be very useful for clinical evaluation.

Concerning the parameters used in this study, it should be noted that for all simulated cases, differences in the stress state were due solely to differences in the geometry of the PPH, since the materials used, the boundary conditions, and the geometry and position of the rest of foot skeleton were the same for all simulated cases. This assumption was adopted in order to isolate the influence of PPH geometry from other factors. On this basis, the same load condition was estimated for the female skeletons as was used for the male skeletons. As bone density is lower in women compared to men [5], in the same way that women's feet are smaller [41] and support lower body weight, the value of the load for women should be increased to match these factors, in a way that maintains the rate of load vs. the degree to which the female foot is able to withstand the load. That configuration is reasonable considering that the results of the simulation were limited to a qualitative comparison between the cases analyzed. Such assumptions had no influence on the stress distribution pattern of the model, where tensile stresses predominated on the lateral side while compressive stresses predominated on the medial side of the PPH.

Our study had several limitations. The fat surrounding the skeleton was not simulated, although all other soft tissues that interact with the skeleton were taken into account. The results obtained from the model, however, were only applicable to hard tissue since, although the model contained some soft tissue, it was simulated in a very simplified and idealized manner and only introduced into the model to create a more realistic environment for the bone structure. This assumption was considered adequate as bone is much harder than soft tissue, and the goal of the study was to analyze the state of the PPH under stress. In addition, we performed a quasi-static analysis as we were only interested in analyzing an isolated phase of gait in which the weight of the body rested on the metatarsal heads. This is the position where the phalanx withstands greater forces. Further development of the model is currently underway in order to include all of the tissues in more detail.

We advise caution when comparing the results obtained from our model with other studies. The current technology is not able to measure the stress within bone, so the results cannot be compared directly with experimental measures. Another option involves comparison with other FE models of the foot. In this regard, however, the reader should beware of comparing stress values between different FE models. This is not a trivial matter. The simplifications, assumptions, and boundary conditions influence the values predicted which makes direct comparison of the results from different FE models almost impossible. Furthermore, to the authors' knowledge, there is no previous FE model which has reported values of bone stress in the toe-off position. Most prior studies only measured values of plantar pressure [8, 10, 36] and rarely in toe-off position [1, 7, 17]. In addition, usually only von Mises stresses were reported, but we felt that for the purpose of analysis of bone, maximum and minimum stresses were more accurate than von Mises stresses, particularly in this study where we attempted to distinguish between tensile and compressive stresses.

5 Conclusions

The present study proposed a new skeletal parameter involved in HAV. The geometry of the PPH has the feature of a larger medial compared with lateral side, subjecting it to stresses that could provoke rotation of the PPH toward a more relaxed position. That potential balanced position produced a tendency toward separation of the first metatarsal relative to the original anatomical position, which constituted the beginning of the HAV deformity.

The data gathered from the dissection showed that the difference in length between the medial and proximal side is greater in women. This suggests that sexual dimorphism of the PPH could be an influential factor in the formation of bunions, with women more prone to suffer this pathology.

The geometry of the PPH is a significant factor in the development of HAV, with as much influence as the other reported skeletal parameters, and should be considered during preoperative evaluation. Therefore, the clinical assessment of HAV should involve evaluation of the first ray as a whole and not as insolated factors.

References

1. Actis RL, Ventura LB, Smith KE et al (2006) Numerical simulation of the plantar pressure distribution in the diabetic foot during the push-off stance. Med Biol Eng Comput 44:653–663. doi:10.1007/s11517-006-0078-5
2. Arinci Incel N, Genç H, Erdem HR, Yorgancioglu ZR (2003) Muscle imbalance in hallux valgus: an electromyographic study. Am J Phys Med Rehabil 82:345–349. doi:10.1097/01.PHM.0000064718.24109.26
3. Barnicott NA, Hardy RH (1955) The position of the hallux in West Africans. J Anat 89:355–361
4. Bayod J, Losa-Iglesias M, Becerro de Bengoa-Vallejo R et al (2010) Advantages and drawbacks of proximal interphalangeal joint fusion versus flexor tendon transfer in the correction of hammer and claw toe deformity. A finite-element study. J Biomech Eng 132(5):51002–51007
5. Berntsen GKR, Fonnebo V, Tollan A et al (2001) Forearm bone mineral density by age in 7, 620 men and women the Tromsø study, a population-based study. Am J Epidemiol 153:465–473
6. Bryant A, Tinley P, Singer K (2000) A comparison of radiographic measurements in normal, hallux valgus, and hallux limitus feet. J Foot Ankle Surg 39:39–43. doi:10.1016/S1067-2516(00)80062-9
7. Budhabhatti SP, Erdemir A, Petre M et al (2007) Finite element modeling of the first ray of the foot: a tool for the design of interventions. J Biomech Eng 129:750–756. doi:10.1115/1.2768108
8. Chen W-M, Lee T, Lee PV-S et al (2010) Effects of internal stress concentrations in plantar soft-tissue—a preliminary three-dimensional finite element analysis. Med Eng Phys 32:324–331. doi:10.1016/j.medengphy.2010.01.001
9. Cheung JT-M, Nigg BM (2008) Clinical applications of computational simulation of foot and ankle. Sport Sport Sport Orthop Traumatol 23:264–271. doi:10.1016/j.orthtr.2007.11.001
10. Cheung JT-M, Zhang M, Leung AK-L, Fan Y-B (2005) Three-dimensional finite element analysis of the foot during standing—a material sensitivity study. J Biomech 38:1045–1054. doi:10.1016/j.jbiomech.2004.05.035
11. Coughlin MJ (1984) Hallux valgus—causes, evaluation, and treatment. Postgrad Med 75:174
12. Duda GN, Mandruzzato F, Heller M et al (2001) Mechanical boundary conditions of fracture healing: borderline indications in the treatment of unreamed tibial nailing. J Biomech 34:639–650. doi:10.1016/s0021-9290(00)00237-2
13. Ferrari J, Hopkinson DA, Linney AD (2004) Size and shape differences between male and female foot bones: Is the female foot predisposed to hallux abducto valgus deformity? J Am Podiatr Med Assoc 94:434–452
14. García-Aznar JM, Bayod J, Rosas A et al (2009) Load transfer mechanism for different metatarsal geometries: a finite element study. J Biomech Eng 131:021011. doi:10.1115/1.3005174
15. García-González A, Bayod J, Prados-Frutos JC et al (2009) Finite-element simulation of flexor digitorum longus or flexor digitorum brevis tendon transfer for the treatment of claw toe deformity. J Biomech 42:1697–1704. doi:10.1016/j.jbiomech.2009.04.031
16. Gefen A (2002) Stress analysis of the standing foot following surgical plantar fascia release. J Biomech 35:629–637. doi:10.1016/s0021-9290(01)00242-1
17. Gefen A, Megido-Ravid M, Itzchak Y, Arcan M (2000) Biomechanical analysis of the three-dimensional foot structure during gait: a basic tool for clinical applications. J Biomech Eng 122:630–639
18. Hardy RH, Clapham JCR (1951) Observations on hallux valgus. J Bone Jt Surg Br 33-B:376–391
19. Heden RI, Sorto LA (1981) The Buckle point and the metatarsal protrusion's relationship to hallux valgus. J Am Podiatry Assoc 71:200–208
20. Helal B (1981) Surgery for adolescent Hallux valgus. Clin Orthop Relat Res (157):50–63
21. Iida M, Basmajian JV (1974) Electromyography of hallux valgus. Clin Orthop Relat Res (101):220–224
22. Johnston O (1959) Further studies of the inheritance of hand and foot anomalies. Clin Orthop 8:146–159
23. Kato T, Watanabe S (1981) The etiology of hallux valgus in Japan. Clin Orthop Relat Res 157:78–81
24. Lamur KS, Huson A, Snijders CJ, Stoeckart R (1996) Geometric data of hallux valgus feet. Foot Ankle Int 17:548–554
25. Laporta G, Melillo T, Olinsky D (1974) X-ray evaluation of hallux abducto valgus deformity. J Am Podiatry Assoc 64:544–566
26. Lundberg BJ, Sulja T (1972) Skeletal parameters in the hallux valgus foot. Acta Orthop 43:576–582. doi:10.3109/17453677208991280
27. Maganaris CN, Paul JP (1999) In vivo human tendon mechanical properties. J Physiol 521:307–313. doi:10.1111/j.1469-7793.1999.00307.x
28. Mancuso JE, Abramow SP, Landsman MJ et al (2003) The zero-plus first metatarsal and its relationship to bunion deformity. J Foot Ankle Surg 42:319–326. doi:10.1053/j.jfas.2003.09.001
29. Mann RA, Coughlin MJ (1981) Hallux valgus-etiology, anatomy, treatment and surgical considerations. Clin Orthop Relat Res 157:31–41
30. Matzaroglou C, Bougas P, Panagiotopoulos E et al (2010) Ninety-degree chevron osteotomy for correction of hallux valgus deformity: clinical data and finite element analysis. Open Orthop J 4:152–156
31. Munuera P, Polo J, Rebollo J (2008) Length of the first metatarsal and hallux in hallux valgus in the initial stage. Int Orthop 32:489–495. doi:10.1007/s00264-007-0350-9
32. Nix S, Smith M, Vicenzino B (2010) Prevalence of hallux valgus in the general population: a systematic review and meta-analysis. J Foot Ankle Res. doi:10.1186/1757-1146-3-21
33. Root ML, Weed JH, Orien WP (1977) Normal and abnormal function of the foot. Clinical Biomechanics, vol 2. Clinical Biomechanics Corporation, Los Angeles
34. Shimazaki K, Takebe K (1981) Investigations on the origin of hallux valgus by electromyographic analysis. Kobe J Med Sci 27:139–158
35. Sim-Fook LAM, Hodgson AR (1958) A comparison of foot forms among the non-shoe and shoe-wearing Chinese population. J Bone Jt Surg 40:1058–1062
36. Takahashi A, Suzuki J, Takemura H (2012) Finite element modeling and simulation of human gait with a spontaneous plantar flexion. Int J Aerosp Light Struct 02:171–185. doi:10.3850/S2010428612000311
37. Tanaka Y, Takakura Y, Kumai T et al (1995) Radiographic analysis of hallux valgus. A two-dimensional coordinate system. J Bone Jt Surg 77:205–213
38. Tao K, Wang C-T, Wang D-M, Wang X (2005) Primary analysis of the first ray using a 3-dimension finite element foot model. In: Conference proceedings IEEE engineering medicine biological society Shanghai, China, pp 2946–9
39. Viladot A (1973) Metatarsalgia due to biomechanical alterations of the forefoot. Orthop Clin North Am 4:165–178
40. Wu KK (1987) Mitchell bunionectomy: an analysis of four hundred and thirty personal cases. J Foot Surg 26:277–292
41. Wunderlich RE, Cavanagh PR (2001) Gender differences in adult foot shape: implications for shoe design. Med Sci Sports Exerc 33:605–611